# Electric Fields in HVDC Paper-Insulated Cables

M. J. P. Jeroense and P. H. F. Morshuis
High Voltage Laboratory, Delft University of Technology, Delft, The Netherlands

## ABSTRACT

**HVDC cables start playing a more and more important role in interconnecting national grids. This paper deals with the calculation of electric fields in HVDC cables. The calculation of fields in an HVDC cable is far more complex than the equivalent case in HV ac cables. This is due to the fact that the conductivity of the cable insulation is temperature and field dependent and due to the fact that the electric fields under dc voltage may be time-dependent. The field distribution in an HVDC cable may be of a capacitive, intermediate (and time-dependent) or resistive nature. The kind of field depends on the stage the cable finds itself in: for instance, whether the voltage has just been applied, whether a polarity reversal has occurred or whether the field distribution has become stable. For each stage, the method of calculating, together with the computed results on a real HVDC cable are discussed. Usually, the effect of heating of the insulation by the leakage current may be disregarded. However, in certain cases, i.e. the cable temperature and applied voltage are high enough, the field distribution is influenced by these insulation losses. They even may lead to an instability that causes breakdown of the cable. A cable in service may be subjected to impulses superimposed on the dc voltage. The most severe case is that of an impulse superimposed on a dc voltage of opposite polarity. The calculation of the field distribution in this situation also is carried out.**

## 1 INTRODUCTION

With common energy resources becoming more and more scarce and with nuclear energy still in a position of social disadvantage, green energy becomes an important issue nowadays. In Europe green energy resources like hydro-electric energy can be found in huge amounts in Scandinavian countries. In a growing number of cases it is preferable to import this type of energy from a Scandinavian country to the European mainland, instead of building new coal or nuclear power stations. The electric energy is transported mostly by submarine power cables at dc voltage. The reason for using dc is the extreme length over which the energy has to be transported; the length can be hundreds of kilometers. The capacitive loading current would be too high when using ac voltage [1]. Another reason for introducing electric links between different countries is the reduction of the necessary number of power plants in Europe by interconnecting the different sub-international grids. Fewer installed power plants can be preferable for economical and environmental reasons. It must be noted that an HVDC cable is not always necessary to reach this latter goal. In several cases a so-called back-to-back connection can do the job. However, in all cases where a large sea has to be crossed, the HVDC cable is the only alternative for interconnecting countries. So far, the paper-insulated HVDC cable is the only type that is in commercial use, due to the high availability of a link that uses such a cable. The paper cables that are used for dc energy transport are mass-impregnated, oil-filled and, very rarely, gas-pressure cables. The polymeric HVDC cable is still in development. This paper deals with the paper insulated cable only. There is a backlog of knowledge concerning the HVDC cable when compared with ac cables. A possible explanation of this backlog is given in [1, 2]. In 1993 a project was started in Delft in order to reduce this lack of knowledge. The project consists of three parts: electric field calculation, space charge measurements and partial discharge measurements [1]. This article deals with the electric field calculation in paper insulated cables. Quantitative knowledge of the electric field is desirable, because the magnitude of the electric field is an important design parameter of a cable. A dc cable can not only experience dc voltages but also ac voltages, impulse and switching surges. All these voltage types may occur superimposed on a dc voltage as well. Therefore, calculation of the electric field in an HVDC cable involves more than just determining the stable dc field. Special attention is given in this paper to the case where the heating of the insulation by the leakage current no longer can be ignored. The new aspect is that it presents calculation methods and results for all possible voltage stages that an HVDC cable may experience.

## 2 DIFFERENCE BETWEEN ac AND dc FIELD CALCULATION IN CABLES

The calculation of electric fields in ac cables is relatively easy. The field distribution depends on the permittivity $\varepsilon_r$ of the insulation material, the geometry of the cable and the applied voltage. The geometry

1070-9878/98/ $3.00 © 1998 IEEE

is in most cases cylindrical. The permittivity to a high extent is independent of external parameters like for instance temperature, at least within the service range (0 to 90°C). In most cases the insulation of an ac cable consists of one material, and the permittivity drops out of the equation determining the field distribution

$$E(r) = \frac{U}{r \ln \frac{R_o}{R_i}} \tag{1}$$

in which $U$ stands for the applied voltage, $r$ the radius in the insulation, $R_o$ the external radius of the insulation and $R_i$ is the internal radius of the insulation. See also Figure 1. The calculation of electric fields in cables under dc voltage is more complex. The field distribution now depends on the permittivity $\varepsilon_r$, the conductivity $\sigma$, the geometry of the cable and the applied voltage $U$. The conductivity depends highly on temperature $T$ and electric field $E$. Many researchers over the world [3–10] came to the conclusion that the conductivity $\sigma$ of impregnated paper insulation can be described by an empirical formula, which is given by

$$\sigma = \sigma_0 \exp(\alpha T) \exp(\gamma E) \tag{2}$$

in which $\sigma_0$ stands for the conductivity at a temperature of 0°C and a field strength of 0 kV/mm, $\alpha$ is the temperature dependency coefficient and $\gamma$ denotes the field dependency coefficient. For mass-impregnated paper the temperature coefficient $\alpha$ normally has a value $\sim$0.1℃ and the field dependency coefficient $\gamma$ normally has a value $\sim$0.03 mm/kV. In a cylindrical structure like a cable, the highest field strength without a load is found near the conductor. The effect of the temperature dependency of the insulation when the cable is loaded is an inversion of the field: the highest field strength is now found near the lead sheath of the cable (see Figure 2). The effect of the field dependency of the insulation is a leveling of the field strength as can be seen in Figure 2.

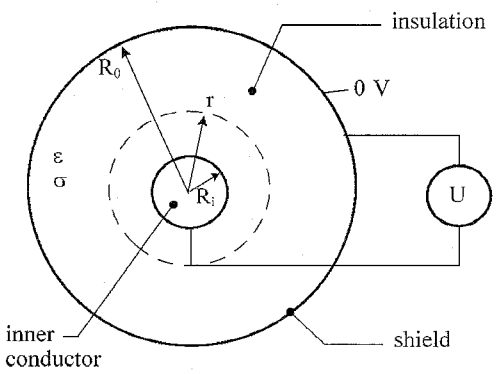


Figure 1. Simplified representation of the cable as it is used to calculate the different electric fields.

Another important fact is that after voltage application there is no dc field distribution in the cable yet. The distribution is at first a capacitive one. Via an intermediate time-dependent field, the distribution changes from the purely capacitive distribution to a purely resistive distribution. To be exact: the purely resistive stage will be reached only after an infinite time! After for instance a polarity reversal, yet another field distribution is found in the cable. Therefore, because the field distributions differ per stage, different computational schemes must be used for every stage that a cable finds itself in.

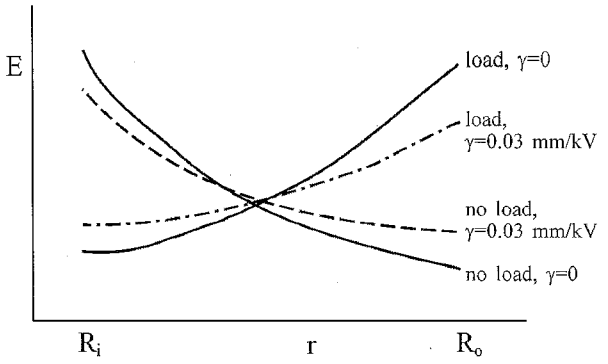


Figure 2. Stable dc fields under load and no-load conditions. The solid lines represent the fields if the field dependency of $\sigma$ is disregarded, the dotted lines represent the fields when taking this effect into account as well.

## 3 DEFINITION OF STAGES

The different stages are described using Figure 3, following the proposal of Kreuger [2]. Focusing on the upper part of the Figure, we see that in stage I, the external voltage $U$ is raised. At the beginning of this stage, the cable contains no space charge and there is no temperature drop across the insulation. The electric field is determined by the geometry and the permittivity $\varepsilon$ only. We speak of a capacitive field distribution. During stage II, the voltage $U$ has already reached its final value. The electric field, however, is changing from a capacitive distribution to a resistive distribution. The field during this stage is time-dependent. A pure resistive field exists in stage III. In all these three stages a load current $I$ may be present, that heats the conductor of the cable. If a load current is present in stage III, it is switched off in stage III$^a$, which is a special case of stage III. The voltage is lowered to zero in stage IV. A field still exists after the voltage has been removed. The lower part of Figure 3 shows the stages during (V) and after (VI) a polarity reversal. During stage VII, the field after a polarity reversal has become stable. Software has been written that calculates the field distributions in each of the defined stages for different ambient temperatures, temperature drops, applied voltages, cable geometries, permittivities, conductivities and the dependency coefficients. The distributions are determined as a function of time where appropriate.

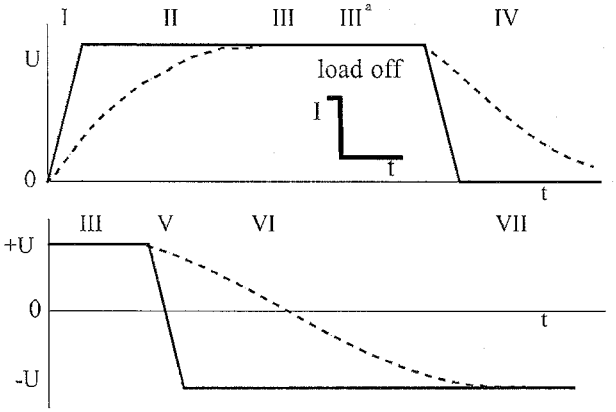


Figure 3. The different stages when switching on and off a dc voltage (top) and after a polarity reversal (bottom). The dotted lines represent the growth and decay of space charges in the insulation.

## 4 FIELDS PER STAGE

In the following sections the field distributions and their method of calculation will be discussed per stage. The calculations will be performed on a 450 kV, 1600 mm$^2$ cable with an inner insulation radius $R_i = 19.2$ mm, an outer insulation radius $R_o = 42.4$ mm, a conductivity $\sigma_0 = 1{\times}10^{-16}\ \Omega^{-1}\mathrm{m}^{-1}$, a relative permittivity $\varepsilon_r = 3.5$ and values of the dependency coefficients $\alpha$ and $\gamma$ as stated earlier. This cable will be named the 'standard' cable. In all calculations the quasi-static approximation will be used, *i.e.* $\nabla{\times}E = 0$.

### 4.1 STAGE I RAISING THE VOLTAGE

In stage I, the external voltage $U$ is raised to its desired value. This takes a short time, usually ~1 s. This time is much shorter than the time constant of the insulation, which is determined by the permittivity $\varepsilon$ and the conductivity $\sigma$ of the insulation. For this reason the field that is present in stage I is a capacitive field. The field may be calculated using Equation (1). This is the same formula as used for ac cables. The field for the standard cable is drawn in Figure 4. It can be seen that the highest field strength is found near the conductor, as known from the ac cables. Equation (1) may be used only if the cable contains no space charge.

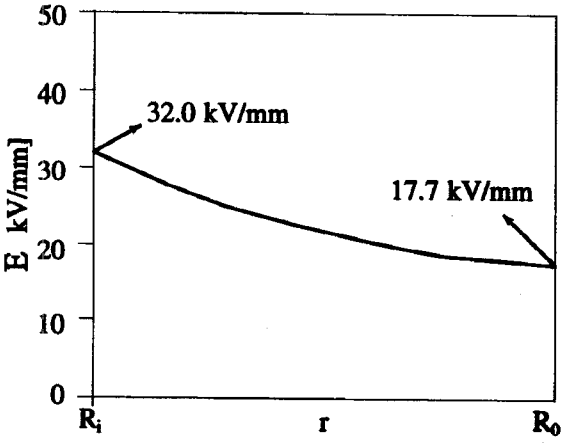


Figure 4. The capacitive field distribution in stage I with $U = 450$ kV.

### 4.2 STAGE II AFTER RAISING THE VOLTAGE

After having raised the voltage (stage I), the field changes from a purely capacitive stage to a purely resistive stage. This Section describes the field between these stages; the field is therefore named an intermediate field.

The field cannot be calculated using an equation in a closed mathematical form. It has to be calculated numerically. The field can be computed using the Gauss law, the continuity equation and Ohms law

$$\nabla \cdot E = \frac{\rho}{\varepsilon} \tag{3}$$

$$\nabla \cdot J + \frac{\partial \rho}{\partial t} = 0 \tag{4}$$

$$J = \sigma E \tag{5}$$

in which $J$ is the current density. Suitable boundary conditions have to be chosen in order to calculate the actual situation: (1) the field distribution $E$ at $t = 0$, (2) the voltage across the insulation is $U$ and the voltage at the lead sheath is 0 V, and (3) a function describing the temperature as a function of radius and time $T(r,t)$. Remember that the conductivity as used in Equation (5) is temperature dependent.

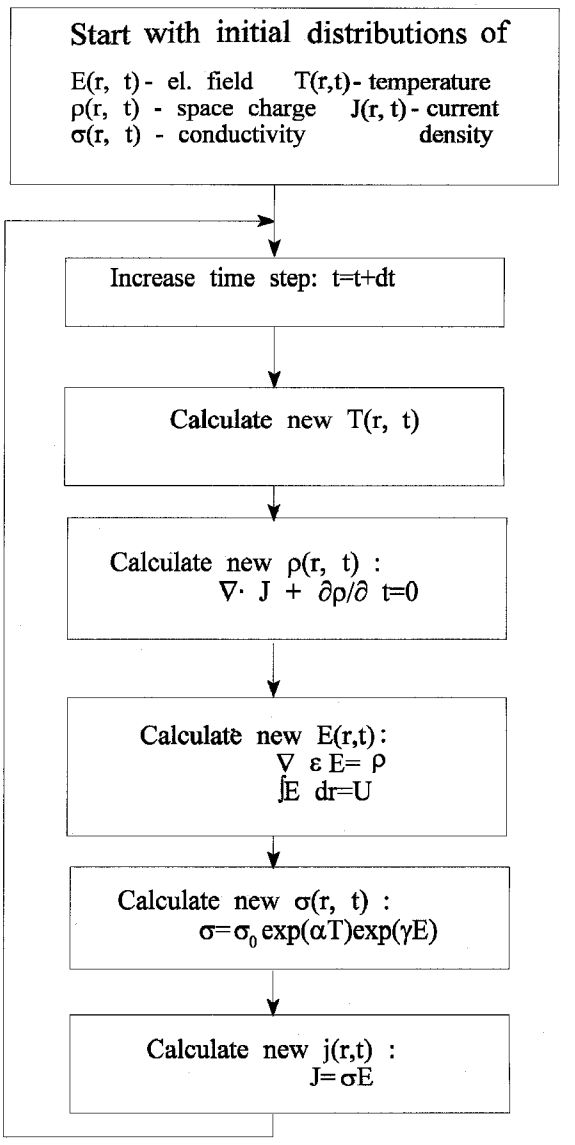


Figure 5. Flow-chart of field-calculating software.

The software calculates the electric field and the charge density by solving these equations in place and time as shown in Figure 5. With regard to the load of the cable, we may calculate three different situations in stage II (see Figure 6).

1. The intermediate field $E$ while the cable is not loaded, $I = 0$.
2. The intermediate field $E$ after the cable has just been loaded.
3. The intermediate field $E$ of a stable loaded cable. The current has been raised long before and the temperature distribution in the cable is stable.

Situation 1 is not very interesting as the field is hardly changing. There is no temperature drop across the insulation, so there will be

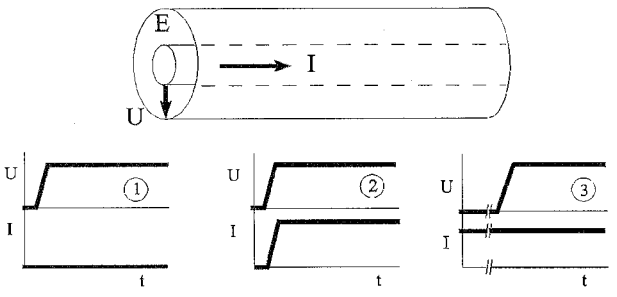


Figure 6. The different situations in stage II as explained in the text.

no field inversion. The field will change slightly due to the field dependency of the conductivity only (compare the lines 'no load, $\gamma = 0.03$ mm/kV' and 'no load, $\gamma = 0$' in Figure 1). Situations 2 and 3 are more interesting because of the field inversion. The intermediate fields in these two situations are almost the same and change from a purely capacitive field to the inverted resistive field. They differ in the rate of change only.

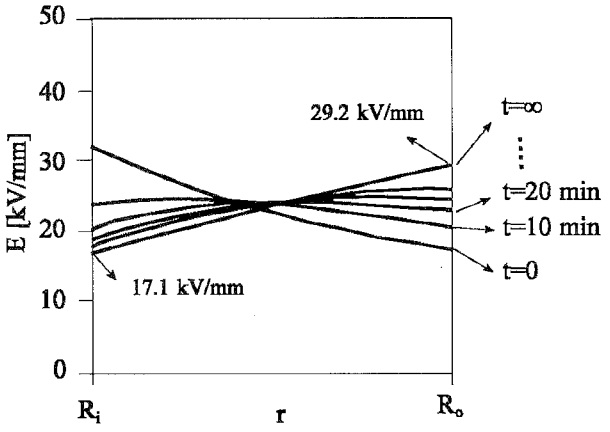


Figure 7. Field distributions in stage II with $U = 450$ kV, $T_s = T_{R_o} = 35$℃ and $\Delta T = T_{R_i} - T_s = 15$℃.

For further explanation we limit ourselves to situation 3.

Figure 7 shows the field distribution in the standard cable at different times. The lead sheath at $R_o$ has a stable temperature $T_s = 35$℃ and a temperature drop $\Delta T = 15$℃ across the insulation. At $t = 0$ the voltage was switched on and resulted in a capacitive field distribution: stage I. The intermediate field is shown for 10 min intervals. The purely resistive field is represented by the line at $t = \infty$. The intermediate fields show that there is a point in the cable, roughly in the middle, where the field is hardly changing. The field at the conductor is decreasing more quickly than the field at the lead sheath is increasing. This is explained by the fact that the insulation near the conductor is 15℃ warmer than the insulation near the lead sheath and has therefore a higher conductivity; the time constant near the conductor is then smaller.

The time constant of a dielectric that consists of two materials with different permittivities $\varepsilon$ or conductivities $\sigma$ is relatively easy to determine [1, 2, 11]. The case of an actual cable is more complex, because the conductivity depends on place and time.

To get an idea of the time constants, the time $t_{63}$ at which the field has changed by 63% is considered. This time is calculated for the change in the field at a point in the insulation adjacent to the conductor and for a point adjacent to the lead sheath. The temperature drop across the insulation was 15℃ and the external voltage was 450 kV. The calculation was performed using different lead sheath temperatures $T_s$. The results are represented by the straight line in Figure 8. It is concluded that the time $t_{63}$ is lower for the insulation near the conductor. This is understandable, as the temperature and therefore the conductivity is higher near the conductor. Further, the time constant is exponentially inversely proportional to the temperature of the cable. The higher the temperature, the shorter the time constant. Observe that the calculations of the time constant have to do with the electric time constant of the cable only, because a stable temperature distribution was taken as starting-point. If the temperature is changing (for instance during heating or cooling of the cable) the thermal time constant of the cable and its environment takes part in the process as well.

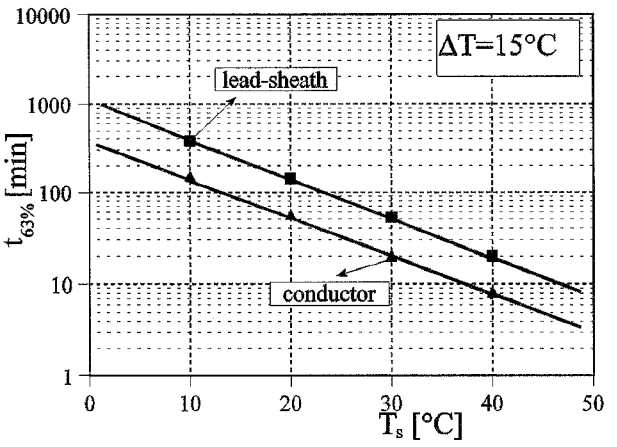


Figure 8. Calculated time spans at which the field has changed for 63% for the model cable.

## 4.3 STAGE III STABLE FIELD

In stage III, the field distribution has become a stable resistive distribution; the field is not time dependent. Due to the temperature dependency and the field dependency, there is a gradient in the conductivity. If such a gradient in the insulation occurs, a space charge is present as may be derived from the Maxwell equations [2, 11]. The space charge generates a field, commonly named the charge-induced field. This charge-induced field causes field inversion and the effect of leveling which have been shown in Figure 1.

First, we start with the calculation of the field, second, we calculate the total insulation resistance of the cable and third, we calculate the space charge distribution.

### 4.3.1 FIELD

The exact electric field including the effect of temperature and field dependence is given by [1]

$$E(r) = U \frac{r^{k-1} \exp(-\gamma E)}{\int_{R_i}^{R_o} r^{k-1} \exp(-\gamma E) dr} \tag{6}$$

in which $k$ is

$$k = \frac{\alpha \Delta T}{\ln\left(\frac{R_o}{R_i}\right)} \tag{7}$$

This equation can be calculated in a numerical way only, because the electric field strength appears at both sides of the equation. In Figure 9, the electric field is calculated for different temperature drops $\Delta T$. With no temperature drop, the highest field strength is found near the conductor: 29 kV/mm (calculated with the data of the standard cable). For large temperature drops (>15°C), the field near the lead sheath may become higher than the highest possible field strength near the conductor. In the middle of the insulation, a point is found where the field is not influenced by the temperature drop.

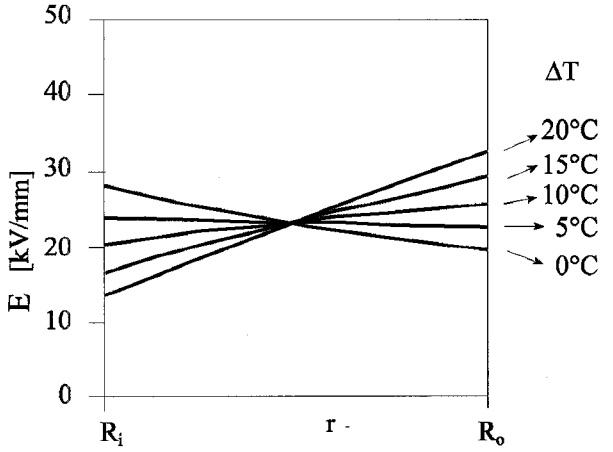


Figure 9. Electric field in the cable insulation in stage III for different temperature drops. The voltage $U = 450$ kV.

From Equations (6) and (7) it is derived that the field distribution does not depend on the absolute temperature but on the temperature drop only. (This holds only if the small influence of ohmic losses due to the leakage current is not taken into account, see Section 5). If we disregard the field dependency $\gamma$ of the conductivity, the field may be calculated analytically. Starting from Equation (6) and setting $\gamma = 0$ we find

$$E(r) = U \frac{r^{k-1}}{\int_{R_i}^{R_o} r^{k-1} dr} \tag{8}$$

which may be written as

$$E(r) = U \frac{k}{R_o \left[1 - \left(\frac{R_i}{R_o}\right)^k\right]} \left(\frac{r}{R_o}\right)^{k-1} \tag{9}$$

From Equation (9) it is seen that the stress distribution varies with $r^{k-1}$. It means that for $k = 0$ (*i.e.* no temperature drop), the distribution is a hyperbolic function like in the capacitive stage. For $k = 1$, the stress distribution is linear and does not depend on the radius. For values of $k > 1$, the stress is inverted. Equation (9) is the approximation used to calculate the dc field taking into account the temperature dependency, but disregarding the field dependency. This approximation is commonly used and is also found in literature [3, 5, 7]. However, care must be taken if the approximation gives large errors for high field strengths and for high temperature drops. In these cases, the leveling effect of the field dependency can no longer be ignored. The error made when using the approximation on the standard cable is shown in Figure 10. The absolute value of the error is calculated for the field near the conductor, and near the lead sheath for different voltages and temperature drops. The error at the conductor is always larger than the error at the lead sheath. The error for a temperature drop $\Delta T = 10$°C is the smallest when the field distribution is almost flat.

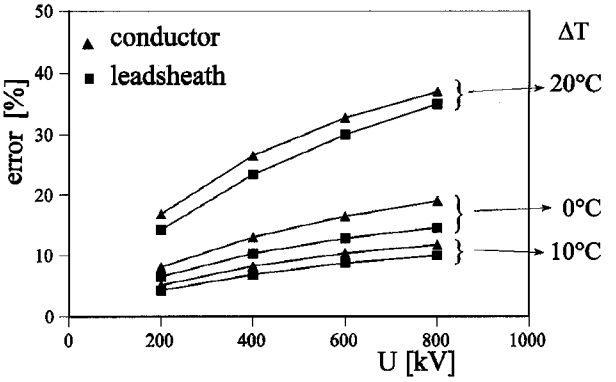


Figure 10. Error in field calculation when using the approximation, Equation (9), instead of Equation (6).

### 4.3.2 RESISTANCE

As the conductivity of the insulation is temperature and field dependent, the total resistance of the cable depends on temperature and field as well. The total resistance per meter cable, taking into account both temperature and field dependency is given by [1]

$$R_{tot} = \frac{\exp(-\alpha T_s)}{2\pi\sigma_0 R_o^k} \int_{R_i}^{R_o} r^{k-1} \exp(-\gamma E) dr \tag{10}$$

in which $T_s$ is the temperature of the lead sheath. From this Equation, it is seen that the total resistance of the cable depends exponentially on the absolute temperature of the cable. This Equation can only be calculated numerically. Disregarding the effect of the field dependency by setting $\gamma = 0$, we can write the equation in a closed analytical form. The resistance per meter cable then becomes

$$R_{tot} = \frac{\exp(-\alpha T_s)}{2\pi\sigma_0 k} \left[1 - \left(\frac{R_i}{R_o}\right)^k\right] \tag{11}$$

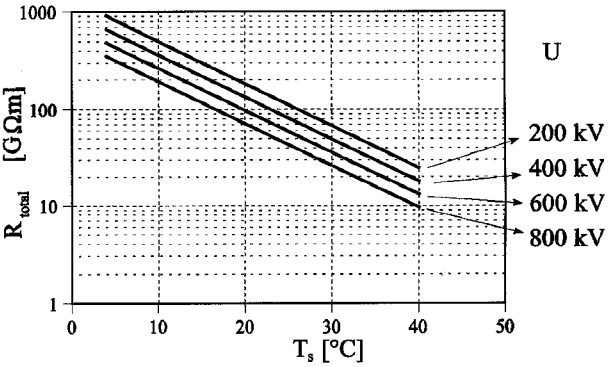


Figure 11. Total resistance per meter cable for different voltages $U$ and lead sheath temperatures $T_s$.

But remember that this equation is an approximation! The resistance per meter standard cable using Equation (10) are shown in Figure 11. From these results we conclude that the total resistance of an HVDC cable can be calculated easily. The total resistance depends exponentially on temperature and linearly on the applied voltage. The higher the applied voltage, the lower the total insulation resistance of the cable.

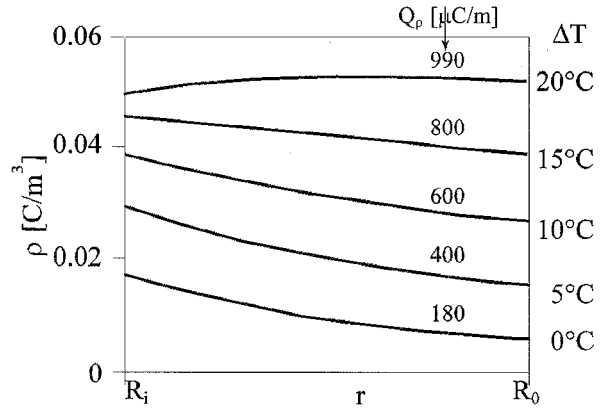


Figure 12. Charge distribution in the standard cable during stage III for different temperature drops $\Delta T$. The voltage $U = 450$ kV.

### 4.3.3 CHARGE

Space charge will be present in the insulation due to the temperature and field dependencies. This type of charge is not trapped charge, but charge that accumulates at discontinuities of permittivity and conductivity. In that case, it must be possible to calculate the charge distribution in the insulation. The space charge distribution in a cable may be calculated using [2]

$$\rho = J \cdot \nabla \frac{\varepsilon}{\sigma} \tag{12}$$

and

$$J = \sigma E \tag{13}$$

in which $J$ is the current density. This equation can be calculated using numerical methods only. The software as described under stage II has been used. Charge distributions in the standard cable at different temperature drops and at 450 kV are given in Figure 12. For the lower temperature drops $\Delta T$, the highest charge densities are found near the conductor. However, the higher the temperature drop, the more the charge will be pushed towards the lead sheath. The charge distribution in the case that $\Delta T = 0$°C is due to the field dependency of the insulation only. Observe that the polarity of the charge is of one sign only. The total charge $Q_\rho$ per meter cable is indicated in this Figure as well. It has been calculated using

$$Q_\rho = \int_{R_i}^{R_o} 2\pi r \rho dr \tag{14}$$

When the field dependency is disregarded, an approximation in calculating the space charge $\rho$ can be made. The calculation may be found in [2], the final result is written as

$$\rho = \varepsilon k \frac{E}{r} \tag{15}$$

Just as in the case of the field approximations, care has to be taken because the error may go up to 50%, especially for higher temperature drops and higher field strengths. Starting from Equation (15), which is an approximation, the total charge per meter cable may also be written in a closed analytical form. Using Equation (14) and approximation (15) we find

$$Q_\rho = 2\pi\varepsilon k \int_{R_i}^{R_o} E dr = 2\pi\varepsilon k U \tag{16}$$

The error in the calculated total charge $Q_\rho$ using Equation (16) may now go up to 200%. Anyhow, from Equation (16), we learn that the total charge in the insulation due to the temperature difference is proportional to the voltage $U$ and to the temperature drop $\Delta T$ ($k$ is a function of $\Delta T$).

It is concluded that the charge accumulation due to temperature and field dependencies in an HVDC cable may be calculated easily. The higher the voltage, the higher the total charge per length of cable. The accumulated charge can easily amount to 500 to 1000 $\mu$C/m, which is a considerable amount of charge.

### 4.3.4 STAGE III$^a$ AFTER SWITCHING OFF THE LOAD

A special stage is introduced here: in stage III$^a$ in which the voltage $U$ remains constant but in which the load current $I$ is switched off. The cable will cool down and the temperature drop will decrease to 0°C. As a result, the field distribution will gradually change from the inverted field back to the usual field where the highest field strength is found near the conductor. The field in stage III$^a$ is an intermediate field and is time-dependent. The theory as described under Stage II is applicable. For this reason, we do not go into detail concerning the fields during this stage. The reason for introducing this special stage is that the cable is vulnerable during the cooling down. Partial discharges with an enhanced repetition rate will occur with a possible harmful effect on the cable. An elaborate description of these phenomena during stage III$^a$ can be found in [1, 12].

### 4.3.5 STAGE IV AFTER SWITCHING OFF THE VOLTAGE

In stage IV, the voltage is switched off. After a short time, determined by the cable capacitance and internal resistance of the voltage source, the external voltage is reduced to zero. The field inside the cable, however, may be present for a far longer time, due to the slow decrease of the space charge. The field remaining after switching off the voltage is a purely charge-induced field. Three situations can be distinguished (see Figure 13).

1. The cable was not loaded before switching the voltage off.
2. The cable was loaded before switching off the voltage. The load is not switched off.
3. The cable was loaded before switching off the voltage. The load is switched off as well.

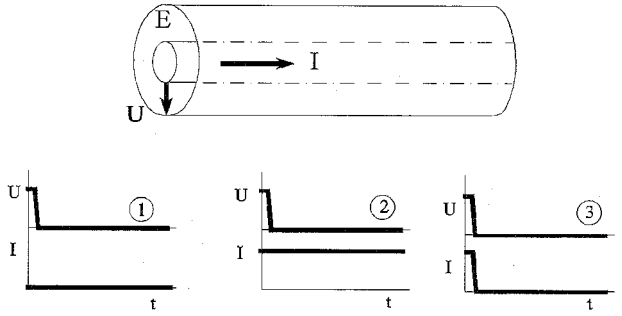


Figure 13. Different situations in stage IV as defined in the text.

If the cable was not loaded earlier (situation 1), the remaining field is not so high because the insulation contained hardly any space charge.

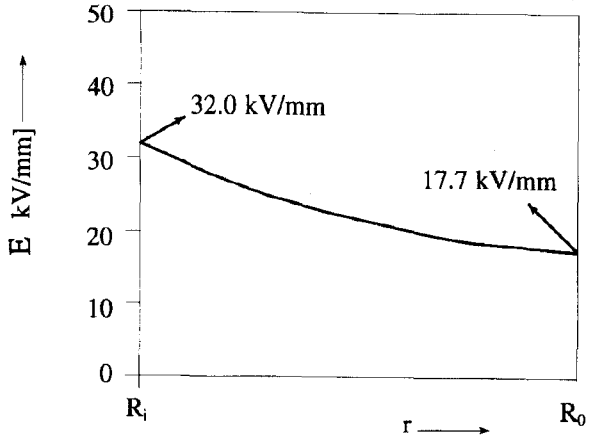


Figure 14. Field distributions after switching off the voltage (stage IV). The voltage before switching it off was 450 kV.

Therefore, situation 1 is not considered here. Situations 2 and 3 give similar decays of the field. In situation 3, the field takes more time to diminish than it does in situation 2, when the temperature is decreasing due to switching off the load. In the following, situation 2 is considered. A cable loaded previously may keep a considerable charge-induced field. As an example, the field distributions of the standard cable after switching off the voltage are shown in Figure 14. The voltage before switching off was 450 kV, whereas the cable is constantly loaded with a current such that the temperature drop $\Delta T = 15$℃. The software introduced under Stage II was used. The field marked with $t = 0^-$ is the field just before switching off the voltage, whereas the field marked with $t = 0^+$ is the field just after switching off the voltage. The other lines represent the field as it decreases in the course of time. The field at $t = 0^+$ just after the voltage has been switched off can be calculated according to

$$E(t = 0^+) = E(t = 0^-) - E_{ac} \tag{17}$$

in which $E_{ac}$ is the capacitive field given by Equation (1) and $E(t = 0^-)$ is the dc field just before switching off the voltage. The field $E(t = 0^+)$ is then the field which is induced by the remaining space charge [1, 2]. Hereafter, the charge-induced field distribution gradually decays until, at $t \to \infty$, the field is 0 kV/mm at every location in the cable.

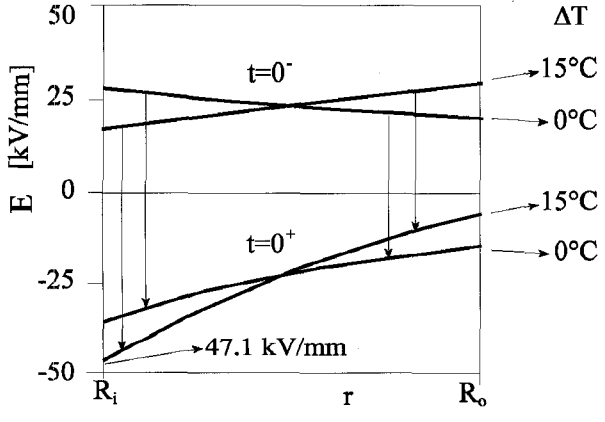


Figure 15. Field distributions before and immediately after a polarity reversal from +450 kV to −450 kV.

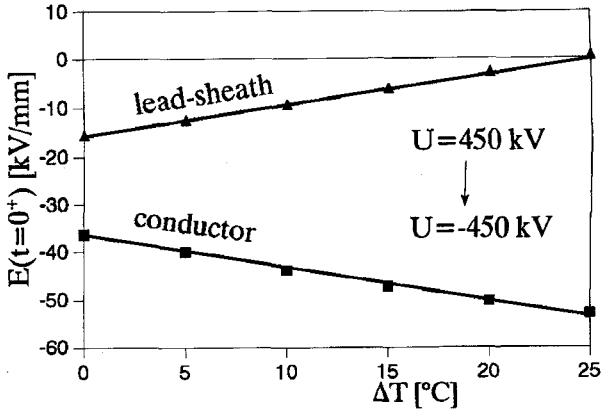


Figure 16. The field at the conductor and the lead sheath immediately after a polarity reversal at different temperature drops $\Delta T$.

### 4.3.6 STAGE V AT POLARITY REVERSAL

It is known that high stresses may occur at the conductor immediately after reversing the polarity of an external voltage source [13]. This is especially the case if the cable is loaded and there is a temperature gradient. This is caused by the space charge of the loaded cable. The field just after the polarity reversal may be calculated in analogy with the theory under Stage IV, with Equation (17) in which $E_{ac}$ is now twice as large as the field strength as calculated with Equation (1)

$$E_{ac} = \frac{2U}{r \ln\left(\frac{R_o}{R_i}\right)} \tag{18}$$

$E(t = 0^-)$ is the field just prior to polarity reversal and $E(t = 0^+)$ the field just after. As the voltage is quickly changed from $+U$ to $-U$, a swing $E_{ac}$ in the electric field according to (18) occurs. This field is subtracted from the initial field. Two examples are given in Figure 15: one in which the cable is not loaded and one in which the cable is loaded, thus resulting in a temperature drop of 15℃. The initial voltage was 450 kV. After the reversal it was −450 kV. The field at the conductor is the highest after a polarity reversal, whether the cable is loaded or not. The field at the conductor after a polarity reversal of a loaded cable is high (47.1 kV/mm in this case) compared to the usual field strengths in service. Obviously, the field at the conductor just after the reversal is largely affected by the temperature drop $\Delta T$. This has been calculated and is shown in Figure 16. Here the voltage was also reversed from +450 to −450 kV. It can be concluded from this Figure that the field strength at the conductor, immediately after the reversal, increases linearly with the temperature drop, whereas the field at the lead sheath decreases linearly.

If the cable did not suffer from inversion at all, this large field increase would not occur. We now consider what measures should be taken to keep the field inversion as low as possible. Under Stage III, it was stated that parameter $k$ describes the inversion. Keeping $k$ as low as possible results in small field inversions. By using the fact that the heat losses $W_c$ in the conductor may be written as

$$W_c = \frac{2\pi\Delta T}{\rho_{th} \ln\left(\frac{R_o}{R_i}\right)} \tag{19}$$

we rewrite parameter $k$

$$k = \frac{\alpha \Delta T}{\ln\left(\frac{R_o}{R_i}\right)} = \frac{\alpha W_c \rho_{th}}{2\pi} \tag{20}$$

in which $\rho_{th}$ is the specific thermal resistivity of the insulation. The field inversion can be kept as low as possible in three ways:

1. By choosing an insulation material that has a low temperature dependency coefficient $\alpha$.
2. By choosing an insulation material that has a low specific thermal resistance $\rho_{th}$.
3. By reducing the losses produced by the conductor.

The losses are ohmic losses and depend on the current $I$, the electric resistivity of the conductor material $\rho_c$ and the conductor area $A$.

However, the most often used conductor material is copper, which already has a low resistivity. The losses may be reduced by reducing the current $I$, which is not desirable. Increasing the conductor area $A$ is a workable option that will reduce the conductor losses. The increase in conductor area is obviously restricted by the costs per meter cable and by mechanical design restrictions.

### 4.3.7 STAGE VI AFTER POLARITY REVERSAL

In this stage, the field gradually changes from the field as calculated under Stage V, to a stable field gained by the reversed voltage source (stage VII). The field in stage VI is an intermediate field and is time-dependent. The field distributions that are calculated and presented in this Section were computed using the software as introduced under Stage II.

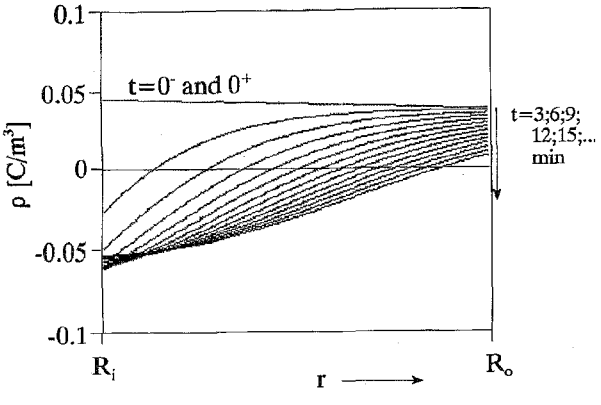


Figure 17. The charge density after a polarity reversal from +450 kV to −450 kV. The temperature drop $\Delta T$ remained stable at 15°C. The temperature of the sheath was 35°C.

We concentrate on the case of a loaded cable, as the highest field strengths occur in that case. Under Stage III (stable field), it was explained that the space charge caused by the dependencies of the insulation was of one sign only: the same polarity as the external voltage. After a polarity reversal, the polarity of the space charge also must reverse. This will happen gradually as shown in Figure 17. The charge distributions in this Figure are a result of a reversal from +450 to −450 kV. The load of the standard cable is not changed, the temperature of the lead sheath is kept constant at 35°C and the temperature drop at 15°C. In Figure 18, the corresponding change in the field distribution is shown.

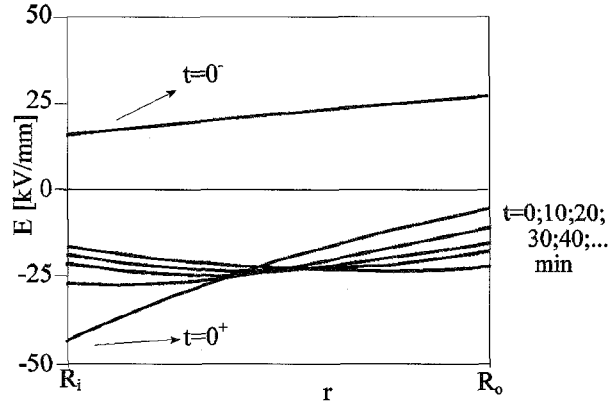


Figure 18. The field distribution after a polarity reversal from +450 kV to −450 kV. The temperature drop $\Delta T$ remained stable at 15°C. The temperature of the sheath was 35°C.

The field strength at the conductor initially is very high, but it decreases quickly. Polarity reversals are severe conditions which, in the recommended tests for HVDC cables, play an important role [13]. It is expected that the ambient temperature has an influence on the decay of the high field strength immediately after a polarity reversal. It is important to know the extent to which the temperature affects the field, as it may make the test more severe. First, the test as recommended by [13] is rewritten. Second, two possible situations are calculated and evaluated.

The polarity reversal as defined in the official recommendations [13] is rephrased below:

> "The cable shall be submitted to a total of 30 daily loading cycles. One cycle consists of 8 h heating, followed by 16 h cooling. Starting with positive voltage, the voltage polarity shall be reversed every 4 h and one reversal shall coincide with the cessation of loading current in every loading cycle. The test voltage shall be $1.5U_0$."

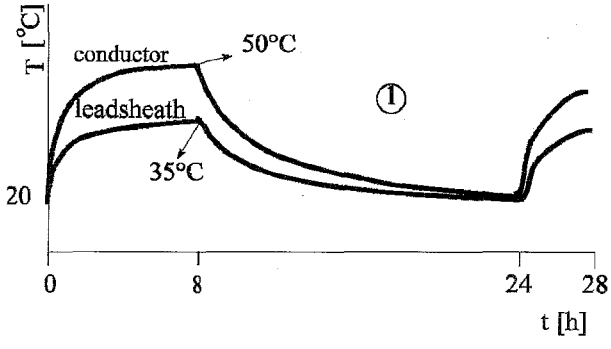


Figure 19. The temperature of the lead sheath and the conductor as a function of time as defined in the text. Situation 1.

The two calculated situations are (see Figures 19 and 20):

(1) A polarity reversal test as defined at an ambient temperature of 20°C (Figure 19). The lead- sheath temperature after 8 h heating is 35°C, the conductor temperature is then 50°C.

(2) The thermal time constant was set to 3 h. At the beginning of the test, the cable was in a stable thermal and electric situation. The voltage on the cable was $1.5 \times 450 = +675$ kV and after reversal $-675$ kV.

(3) A polarity reversal test as defined at an ambient temperature of 4°C (Figure 20). The lead sheath temperature is kept constant at 4°C.

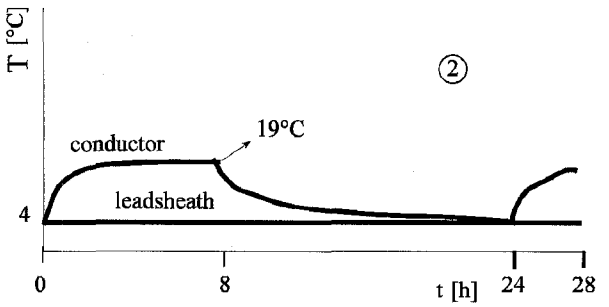


Figure 20. The temperature of the lead sheath and the conductor as a function of time as defined in the text. Situation 2.

The temperature of the conductor after the 8 h heating is 19°C. The thermal time constant was set to 3 h. At the beginning of the test, the cable was in a stable thermal and electric situation. The voltage on the cable before reversal was $1.5{\times}450 = +675$ kV and after reversal $-675$ kV.

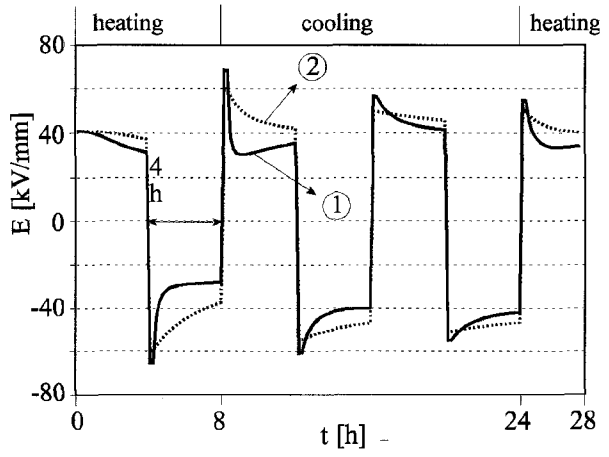


Figure 21. The field at the conductor as a function of time during a polarity reversal test as recommended by [13]. Situation 1: high ambient temperatures. Situation 2: low ambient temperatures.

The results of the calculations of situations 1 and 2 are represented in Figure 21. The Figure shows the field strength at the conductor as a function of time. The high field strength, which is present immediately after the polarity reversal, decays more slowly for the cable in cold environment (situation 2) than for the cable in warm environment (situation 1). It is concluded that, regarding the field strength, testing a cable with polarity reversals and subjection to a low ambient temperature is a more severe test than that of a cable subjected to a high ambient temperature.

### 4.3.8 STAGE VII STABLE AFTER POLARITY REVERSAL

After the intermediate field of stage VI, the field becomes stable in stage VII. The field is of opposite polarity to the field in stage III. All calculations made in stage III are valid for stage VII, but with an opposite sign

$$E_{VII} = -E_{III} \tag{21}$$

## 5 FIELDS TAKING INTO ACCOUNT OHMIC INSULATION LOSSES

The leakage current $I_0$ in the insulation heats the insulation; this is caused by ohmic losses which are of the form

$$w = \frac{I_0^2}{(2\pi r)^2 \sigma} \tag{22}$$

in which $w$ is the power generated per unit volume and $I_0$ is the leakage current per meter cable [1]. Normally, the power generated throughout the whole insulation per meter of cable is in the order of 1 mW, which is small compared to the 25 W per meter of cable which is generated by the conductor. These values are rough figures calculated at a moderate stress and ambient temperature. However, the effect of the ohmic insulation losses may be greater at higher stresses and ambient temperatures. Consider the following. The leakage current will heat the insulation due to the ohmic insulation losses. Therefore, the temperature of the insulation will rise. The higher temperature will lead to an increase in the electrical conductivity. This higher conductivity causes a higher leakage current. However, the higher leakage current will in its turn heat the insulation. The process continues until either a balance is reached or an instable situation occurs [1, 14].

Thus, the electric field may be influenced to a larger extent than one would expect. In the following, the electric field distribution is calculated, taking into account the effect of the ohmic insulation losses. It can be calculated [1] that the temperature drop $T_r - T_c$ at location $r$ inside the insulation due to the heating by the leakage current $I_0$ is given by

$$T_r - T_c = -\rho_{th} I_0^2 \int_{r'=R_i}^{r} \frac{1}{r'} \left( \int_{r''=R_i}^{r'} \frac{dr''}{4\pi^2 (r'')^2 \sigma} \right) dr' \tag{23}$$

in which $T_r$ is the temperature of the insulation at location $r$, $T_c$ is the temperature of the conductor, $\rho_{th}$ is the specific thermal resistance of the insulation which is thought to be independent of temperature, and $\sigma$ is the electric conductivity which depends on the location in the insulation. This temperature drop comes in addition to the well-known temperature drop $\Delta T$ which is the result of the conductor losses. Equation (22) may be used to calculate the electric field. The electric field distribution is calculated in an iterative way:

1. Calculate an initial field (this may be the field calculated with the equations under Stage III).
2. Calculate the temperature distribution using Equation (22).
3. Calculate the distribution of the electric conductivity.
4. Calculate the electric field distribution.
5. Calculate the leakage current $I_0$.

Repeat steps 2 to 5 until the field distribution does not change more than $10^{-2}$ kV/mm. It is possible that this equilibrium situation will not occur and the changes in field of following iterations become larger and larger. This is the instability as mentioned earlier.

The fields were calculated for the cable at $2U_0 = 900$ kV with a current of 1500 A flowing through the conductor of the standard cable. The calculations were done using different lead sheath temperatures $T_s$ to investigate the effect of the ambient temperature. The thermal conductivity $\sigma_{th} = 0.17\,\mathrm{Wm^{-1}K^{-1}}$. The results are shown in Figure 22.

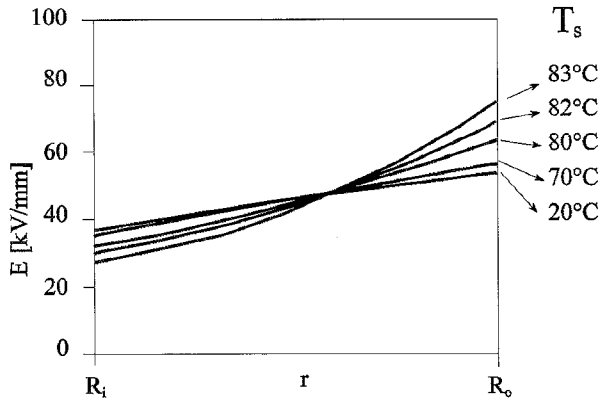


Figure 22. Stable field distributions taking into account ohmic insulation loss for different temperatures of the lead sheath $T_s$. $U = 900$ kV.

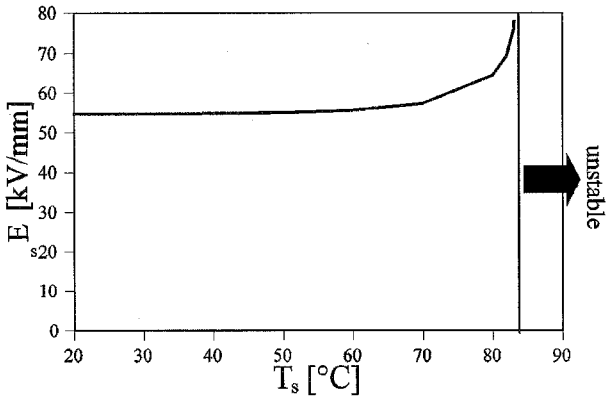


Figure 23. Field $E_s$ at the lead sheath taking into account ohmic insulation loss as a function of the temperature of the lead sheath $T_s$. $U = 900$ kV.

It is seen that the field is pushed still more towards the conductor, but for very high temperatures, >70°C only. This is shown in Figure 23 where the field $E_s$ at the lead sheath is shown as a function of the temperature $T_s$ of the lead sheath. For temperatures of the lead sheath higher than 83°C, no solution exists and instability sets in. As the leakage current $I_0$ is the parameter which causes the deformation of the field, we have a closer look at Figure 24. The relation between the leakage current $I_0$ and the temperature of the lead sheath $T_s$ is exponential. This was expected, as the electric conductivity is exponentially proportional to the temperature. However, several degrees below instability, the leakage current $I_0$ is increasing more than exponentially (indicated by the curved arrow). The power $W_p$ generated by the insulation losses and the power $W_c$ generated by the conductor losses are shown in the same Figure. It is seen that $W_p$ has the same exponential shape as the leakage current $I_0$. For the higher temperatures, the power $W_p$ takes values just as high as the average conductor losses $W_c$ or even more.

Figure 24 shows that at a temperature of the lead sheath $T_s = 70$°C, the power generated by the insulation is $\sim\frac{1}{3}$ of the power generated by a fully loaded conductor ($W_p = 0.3W_c$). The electric field distortion caused by the leakage current becomes important starting at this temperature of 70°C. The conclusions are twofold.

(1) The insulation losses can no longer be disregarded in the cases where $W_p \geqslant 0.3W_c$ ($W_c$ of a fully loaded conductor). This situation

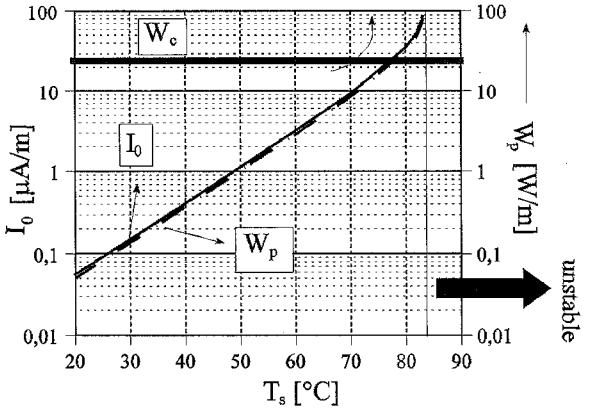


Figure 24. Leakage current per meter cable $I_0$ and power $W_p$ generated by the leakage current as a function of the temperature of the lead sheath $T_s$. $W_c$ is the power generated by the conductor. $U = 900$ kV.

may occur for high lead sheath temperatures and high voltages. The maximum operating temperature of mass-impregnated insulation, however, is ~55°C. The insulation losses may be disregarded under normal service conditions concerning this type of cable. Oil-filled cables, however, may be used at a much higher operating temperature. Consequently, the risk for a thermal breakdown during testing conditions is present.

(2) In laboratory situations and when evaluating new insulation materials at high temperatures, one should be aware of the effect. A risk of instability may then be present.

## 6 IMPULSES SUPERIMPOSED ON DC VOLTAGE

An HVDC cable may suffer from switching and lightning transients. A cable in service experiences these transients superimposed on its own dc voltage. In the following, impulses superimposed on a dc voltage are considered, especially the impulses superimposed on a dc voltage of opposite polarity, to which the cable is most vulnerable [1, 15–17]. First, the definition of symbols is given. $U_{dc}$ is the dc working voltage, $U_p$ is the resulting peak voltage if an impulse is superimposed on the existing dc voltage (see Figure 25). The field at the event of an impulse can be calculated using

$$E_p = E_{dc} + E_{ac} \tag{24}$$

where

$$E_{ac} = \frac{U_p - U_{dc}}{r \ln\left(\frac{R_o}{R_i}\right)} \tag{25}$$

Note that the capacitive field $E_{ac}$ is larger for superimposed impulses of opposite polarity ($|-U_p - U_{dc}| > |U_p - U_{dc}|$).

As an example, the field at the event of the impulse is calculated for the standard cable at +450 kV with a superimposed impulse of opposite polarity such that $U_p = -1000$ kV. The fields are calculated for an unloaded cable ($\Delta T = 0$) and for a loaded cable ($\Delta T = 15$°C). The result is shown in Figure 26. The field strength at the event of a superimposed impulse is the highest near the conductor, both for a loaded and an unloaded cable. The loaded cable suffers from a higher total field strength $E_p$ than the unloaded cable. In the case of a superimposed impulse of the same polarity, the field strength at the conductor is always

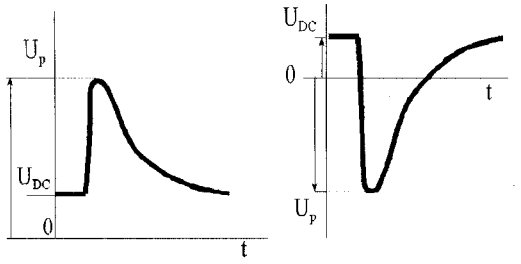


Figure 25. Definition of voltages $U_{dc}$ and $U_p$.

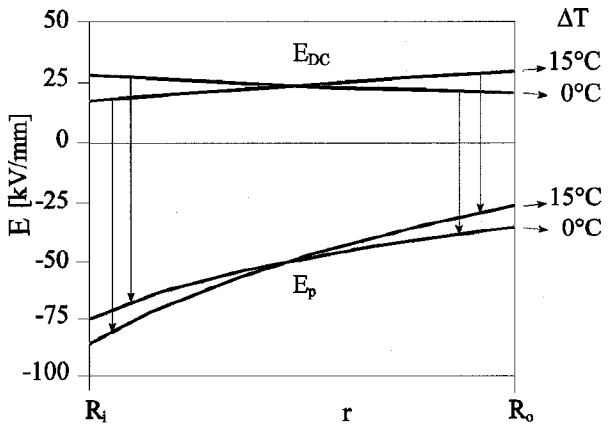


Figure 26. Field distribution at the event of an impulse superimposed on a dc voltage of opposite polarity. $U_{dc} = +450$ kV and $U_p = -1000$ kV.

the highest for an unloaded cable, but may become higher at the lead sheath for high dc voltages when loaded (not shown in the Figure). The field at the conductor $E_c$ in the event of a superimposed impulse is evaluated for several prestressing dc voltages $U_{dc}$ and temperature drops $\Delta T$ in Figure 27. The absolute value of the peak voltage $U_p$ was set to 1000 kV. The magnitude of the field at the conductor is decreasing with increasing dc prestress for impulses superimposed on a dc voltage of the same polarity.

The magnitude of the field is increasing with increasing dc prestress for impulses superimposed on a dc voltage of opposite polarity. Higher temperature drops $\Delta T$ increase the effect. By comparing the field strengths in Figure 27, it is concluded that a test with an impulse superimposed on a dc voltage of opposite polarity (arrow $a$) leads to higher

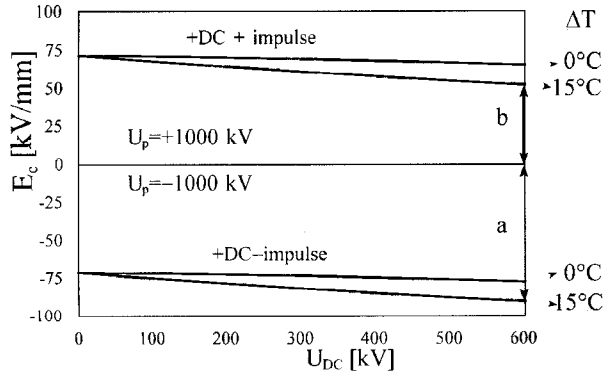


Figure 27. Field at the conductor at the event of an impulse superimposed on a dc voltage of the same and of opposite polarity.

field strengths near the conductor than to a test done with an impulse of the same polarity (arrow $b$) as the dc voltage. On top of this, the breakdown field strength is lower in the case of an impulse superimposed on a dc voltage of opposite polarity than an impulse superimposed on a voltage of the same polarity. This has been found by several authors for mass-impregnated paper cables [16, 17] and for extruded cables [18, 19]. This has two reasons.

(1) The capacitive field during the impulse, described by Equation (24) is larger for the impulse superimposed on a dc voltage of opposite polarity than the capacitive field during a pulse superimposed on a dc voltage of the same polarity. In a mass-impregnated paper the butt gaps are stressed mostly by this capacitive field as they have a lower permittivity $\varepsilon_r$ than the paper. This holds for oil-filled and gas-filled butt gaps. The butt gaps are the weakest points in the cable and will, therefore, suffer more from an impulse superimposed on a dc voltage of opposite polarity.

(2) Mass-impregnated paper cables and extruded cables may contain space charge. In the case of a paper cable, homocharge will be accumulated in the paper layers adjacent to the conductor and lead sheath as shown by Jeroense [1]. Extruded cables also may contain homocharge [18, 19]. At the event of an superimposed impulse of opposite polarity, these homocharges increase the stress in the butt gaps of a paper cable and the interfaces of an extruded cable.

## 7 CONCLUSIONS

THE conduction of the insulation of an HVDC paper insulated cable is time and field dependent. Therefore, the field distributions have to be calculated for each stage that the cable finds itself in. Seven different stages were defined. In each stage, the method of calculation and the results of the computations were discussed. Besides the calculation of the field distributions, the charge distributions are determined per stage. Only in the case of a stable capacitive stage, the field distribution can be calculated analytically. In the resistive stage an approximation can be made by disregarding the field dependency. In that case the resistive field distribution can be calculated analytically. It should be observed that the error, when disregarding the field dependency, may go up to 30%. The intermediate fields change slower in a cold cable than in a warm one. Therefore, testing a cold cable with polarity reversals is a more severe test than testing a warm cable with polarity reversal, regarding the field strength. In cases of a high cable temperature and a high applied voltage, the heating of the insulation by the leakage current cannot be ignored. The field distribution is distorted by the ohmic insulation losses caused by the leakage current. In severe cases this may lead to an instability. Impulses superimposed on a dc voltage of opposite polarity result in higher field strengths near the conductor than impulses superimposed on dc voltages of the same sign. The new points in this paper are found in the fact that it gives calculation methods for all possible voltage stages that an HVDC cable may experience.

## ACKNOWLEDGMENT

This work has been accomplished within the framework of a joint cooperation between the Dutch Cable Factory NKF Kabel BV and Delft University of Technology. We are grateful to NKF in giving us the opportunity to publish these results.

## REFERENCES


[1] M. J. P. Jeroense, *Charges and Discharges in HVDC cables - in particular in impregnated HVDC cables*, thesis, Delft University of Technology, Delft University Press, Delft, 1997.

[2] F. H. Kreuger, *Industrial High DC Voltage*, Delft University Press, Delft, The Netherlands, 1995.

[3] E. Occhini and G. Maschio, "Electrical Characteristics of Oil-Impregnated Paper as Insulation for HV DC Cables", IEEE Trans. Power Apparatus and Systems, Vol. 86, pp. 312–326, 1967.

[4] M. J. P. Jeroense and F. H. Kreuger, "Electrical Conduction in Mass-Impregnated Paper Cable", IEEE Trans. Dielectrics EI, Vol. 2, pp. 718–723, 1995.

[5] J. M. Oudin, M. Fallou and H. Thévenon, "Design and Development of DC Cables", IEEE Trans. Power Apparatus and Systems, Vol. 86, pp. 304–311, 1967.

[6] S. C. Chu, "Design Stresses and Current Ratings of Impregnated Paper Insulated Cables for HV DC", IEEE Trans. on Power Apparatus and Systems, Vol. 86, pp. 1029–1036, 1967.

[7] F. H. Buller, "Calculation of Electrical Stresses in DC Cable Insulation", IEEE Trans. on Power Apparatus and Systems, Vol. 86, pp. 1169–1178, 1967.

[8] F. H. Buller, "Calculation of Electrical Stresses in DC Cable Insulation", IEEE Summer Power Meeting, New Orleans, La., July 1966.

[9] B. R. Nyberg, K. Herstad and K. Bjørløw-Larsen, "Numerical Method for Calculation of Electrical Stresses in HVDC Cables with Special Application to the Skagerrak Cable", IEEE Trans. on Power Apparatus and Systems, Vol. 94, pp. 491–497, 1975.

[10] O. Tollerz, "A 200 km Long Submarine Cable for the Fenno-Skan HVDC link", ABB review, March 1989.

[11] T. Jing, *Surface Charge Accumulation in $SF_6$*, thesis, Delft University of Technology, Delft University Press, Delft, 1993.

[12] A. Eriksson, G. Henning, B. Ekenstierna, U. Axelsson and M. Akke, "Development Work Concerning Testing Procedures of Mass-Impregnated HVDC Cables", CIGRE 21–206, 1994.

[13] CIGRE Working Group 02 of Study Committee No. 21, "Recommendations for Tests of Power Transmission DC Cables for a Rated Voltage up to 600 kV", Electra No. 72, pp. 105–114, 1980.

[14] C. K. Eoll, "Theory of Stress Distribution in Insulation of HV DC Cables: Part I", IEEE Trans. Electr. Ins., Vol. 10, pp. 27–35, 1975.

[15] CIGRE Joint Working Group 33[21]14–16, "Overvoltages on HVDC Cables", Erlangen, April 1994.

[16] G. Bahder, F. G. Garcia and A. S. Brookes, "Insulation Co-ordination in HV dc Cables", CIGRE 21–03, 1972.

[17] G. Maschio and E. Occhini, "HV Direct Current Cables: the State of the Art", CIGRE 21–10, 1974.

[18] M. Pays, M. Louis, J. Perret, C. Alquié and J. Lewiner, "Behavior of extruded HVDC power cables", CIGRE 21–07, 1988.

[19] Y. Maekawa, A. Yamaguchi, C. Ikeda and M. Hara, "Research and Development of DC XLPE Cables", Jicable, B9 Cables and Accessories for HVDC Links - Submarine Cables (1), pp. 562–569, 1991.


*Manuscript was received on 2 December 1997, in revised form 2 March 1998.*